Proc. Natl. Acad. Sci. USA
Vol. 95, pp. 5562–5567, May 1998
Cell Biology

Alzheimer's-specific effects of soluble β-amyloid on protein kinase C-α and -γ degradation in human fibroblasts

ANTONELLA FAVIT, MAURIZIO GRIMALDI, THOMAS J. NELSON, AND DANIEL L. ALKON†

Laboratory of Adaptive Systems, National Institute of Neurological Disorders and Stroke, National Institutes of Health, Bethesda, MD 20892

Communicated by Bernhard Witkop, National Institute of Diabetes, Chevy Chase, MD, March 3, 1998 (received for review December 23, 1997)

ABSTRACT **Alzheimer's disease (AD) is a multifactorial disease in which β-amyloid peptide (βAP) plays a critical role. We report here that the soluble fraction 1–40 of βAP differentially degrades protein kinase C-α and -γ (PKCα and PKCγ) isoenzymes in normal (age-matched controls, AC) and AD fibroblasts most likely through proteolytic cascades. Treatment with nanomolar concentrations of βAP(1–40) induced a 75% decrease in PKCα, but not PKCγ, immunoreactivity in AC fibroblasts. In the AD fibroblasts, a 70% reduction of the PKCγ, but not PKCα, immunoreactivity was observed after βAP treatment. Preincubation of AC or AD fibroblasts with 50 μM lactacystine, a selective proteasome inhibitor, prevented β-AP(1–40)-mediated degradation of PKCα in the AC cells, and PKCγ in the AD fibroblasts. The effects of βAP(1–40) on PKCα in AC fibroblasts were prevented by inhibition of protein synthesis and reversed by PKC activation. A 3-hr treatment with 100 nM phorbol 12-myristate 13-acetate restored the PKCα signal in treated AC cells but it did not reverse the effects of βAP(1–40) on PKCγ in the AD fibroblasts. Pretreatment with the protein synthesis inhibitor, cycloheximide (CHX, 100 μM), inhibited the effects of βAP(1–40) on PKCα and blocked the rescue effect of phorbol 12-myristate 13-acetate in AC fibroblasts but did not modify PKCγ immunoreactivity in AD cells. These results suggest that βAP(1–40) differentially affects PKC regulation in AC and AD cells via proteolytic degradation and that PKC activation exerts a protective role via *de novo* protein synthesis in normal but not AD cells.**

The β-amyloid protein (βAP) is the major constituent of the neuritic plaques that are, together with the neurofibrillar tangles, physiologic hallmarks of Alzheimer's disease (AD) (1, 2).

Excessive release of βAP in different cerebral areas, promoted by a mutant form of amyloid precursor protein (APP), contributes to its accumulation within the neuritic plaques (3, 4). In many cell types from AD tissues, including fibroblasts, changes have been demonstrated in signal transduction systems (5) that involve calcium homeostasis (6–9), ion channel permeability (10–12), cyclic AMP (13, 14), and phosphoinositide metabolites (15). Altered production of βAP also has been shown (16–18). Furthermore, βAP itself can affect the same transduction systems.

Low concentrations (10 nM) of βAP(1–40) can affect K+ channel opening (19) and reduce intracellular levels of GTP-binding proteins (20) in human fibroblasts. Although a biphasic effect of βAP treatment on rat neuronal cell cultures also has been reported (21, 22), the mechanisms underlying the acute effects of βAP, including increased sensitivity to oxidative stress (23, 24), are still not well understood.

Previous demonstrations of PKC deficits in the frontal cortex (25) and alterations in PKC-dependent phosphorylation in the brains of Alzheimer's patients suggested an early role for PKC dysfunction in the pathogenesis of AD (26–31). Furthermore, reduced PKC phosphorylating activity and a lower affinity for phorbol ester binding as well as a decreased PKC immunoreactivity have also been reported for AD fibroblasts (32, 33). In this study, we investigate the acute effects of βAP(1–40) on PKC regulation in Alzheimer's fibroblasts.

MATERIALS AND METHODS

Cell Culture. Human skin fibroblasts were purchased from Coriel Cell Repositories, seeded, and maintained as described (20). Cells from 6 familial AD [AG07872, AG06840B, AG8170B, AG08527A*, AG06848B*, AG08563A; four males and two females, 57.7 ± 2.1 years of age (mean ± SD); *, autopsy confirmation], 4 nonfamilial AD (AG05770D*, AG07377, AG06263, AG06838; two males and two females, 53.8 ± 1.1 years of age; *, autopsy confirmation), 10 age-matched AC (AG07665A, AG06842B, AG07867, AG07603A, AG04560B, AG06241B, AG3652C, AG07141, AG08044A, AG07310; six males and four females, 55.2 ± 2.9 years of age) were used. Passage numbers were almost exactly the same for AC (7.3 ± SD 1.4, $n = 11$) and AD (6.7 ± SD 0.6, $n = 11$) cell lines. There were no differences in growth rates or time to senescence between AD and control fibroblasts (34). Cells were grown to confluence in DMEM (GIBCO) supplemented with 10% fetal bovine serum (GIBCO). Rat cerebellar granule cells were prepared as described previously (35). Briefly, cerebella from 8-day-old rat were dissociated after trypsinization (0.025% trypsin solution) and trituration in the presence of DNase (0.01%) and trypsin inhibitor (0.05%). Cells were then dispersed and cultured into basal medium Eagle's (BME) supplemented with 25 mM KCl/2 mM glutamine/10% fetal bovine serum (GIBCO). The growth of nonneuronal cells was inhibited by the addition of 20 μM cytosine β-D-arabinofuranoside. Cortical neuron cultures were performed as described (36) with slight modifications. Cortical tissue was obtained from fetuses extracted by a C-section from a 17-day pregnant rat. Brains were dissected, dissociated in a solution containing 26 units/mg papain and 1 mM cysteine, and dispersed in DMEM supplemented with 10% fetal bovine serum and 100 units/ml penicillin and 100 μg/ml streptomycin. Cells then were seeded for 72 h before the addition of 1 μM cytosine β-D-arabinofuranoside.

***β*-Amyloid Treatment.** βAP(1–40) (Bachem) was dissolved initially in dimethyl sulfoxide (DMSO, 100 μM) (21, 22) and further diluted in saline solution to desired final concentrations (1 nM–5 μM). βAP(1–40) was added 24 h after seeding

The publication costs of this article were defrayed in part by page charge payment. This article must therefore be hereby marked "*advertisement*" in accordance with 18 U.S.C. §1734 solely to indicate this fact.

0027-8424/98/955562-6$0.00/0
PNAS is available online at http://www.pnas.org.

Abbreviations: AD, Alzheimer's disease; AC, age-matched controls; βAP, beta-amyloid protein; Lacta, lactacystine; CHX, cycloheximide; PMA, phorbol 12-myristate 13-acetate; APP, amyloid precursor protein; DIV, days *in vitro*.

†To whom reprint requests should be addressed at: National Institutes of Health, Building 36, Room 4A-21, Bethesda, MD 20892. e-mail: dalkon@codon.nih.gov.

and DMSO alone was added as vehicle control in all experiments. The total DMSO concentration was <0.1% in both treated [with βAP(1–40)] and nontreated groups (21, 22). Furthermore, there were no apparent differences in any of the measured parameters for DMSO and H_20 vehicle controls. Experiments were conducted starting from 24 to 120 h after addition of βAP(1–40). None of these βAP(1–40) concentrations have been shown to alter basal levels of intracellular calcium or cause other nonspecific cell damage (19).

Protein Extraction. Protein extraction was performed as described previously (20). Briefly, pellets were resuspended in homogenizing buffer containing 0.1 M Hepes, 0.04 M EDTA, 0.8 M sucrose, 0.01 M phenylmethylsulfonyl fluoride (PMSF), 2.4 units/ml aprotinin, and 1% SDS, and sonicated (ultrasonic homogenizer, Cole–Parmer). Protein concentration was determined by an established dye-binding assay (37) for all homogenates. The crude extracts were placed at 4°C right before immunoblotting analysis was performed.

Immunoblotting Analysis. Western blot analysis was performed as described (38). SDS/PAGE was carried out in a 4–20% acrylamide gradient gel of 1.5-mm thickness (NOVEX, San Diego). The crude homogenate was balanced with sample buffer containing 0.5 M Tris·HCl (pH 6.8), 10% glycerol, 2% SDS, and 0.5% 2-mercaptoethanol, to a final volume of 20 μl with a total protein concentration of 10 μg/μl. The samples were electrophoresed and transferred overnight into a nitrocellulose paper (Schleicher & Schuell). The nitrocellulose was blocked in 1% BSA/95% TBS for 1 h and then incubated with different PKC isoenzyme antibodies (PKCα, PKCβ, PKCγ, PKCδ, PKCε mAbs; Transduction Laboratories, Lexington, KY) for 1 h. Blots were then incubated with an anti-mouse alkaline phosphatase-conjugated antibody (Sigma) for 1 h. Finally, the nitrocellulose was stained with a solution containing 0.1 M Tris·HCl (pH 9.6), 0.001 M MgCl, 1% nitroblue tetrazolium (Pierce), and 1% 5-bromo-4-chloro-3-indolyl phosphate toluidine salt (Pierce). All reactions were carried out at room temperature. Immunoblots were digitized on a flatbed scanner and analyzed by quantitative analysis with imaging software written in the laboratory (TNIMAGE by T.J.N.; available by file transfer protocol to las1.ninds.nih.gov) as described previously (20), and measurements of the regions of interest were normalized to the total densitometric area per lane.

Confocal Microscopy. Fibroblasts from AD and control patients were seeded onto a 75-mm × 25-mm × 0.5-mm glass microscope slide and processed to determine the immunofluorescent content of the different PKC isoenzymes. Briefly, cells were fixed with 4% formaldehyde, permeabilized in 0.1% Triton X-100, and incubated with mAbs against different PKC isoenzymes for 40 min. Fibroblasts were then washed and incubated for 20 min in the presence of an anti-mouse antibody conjugated with fluorescein. Finally, the slides were mounted on a coverslip and visualized on a Zeiss inverted laser confocal (39) microscope system by using a ×63 (Neofluar) objective. Four-second activation scans of the fluorescent antibody complex from the upper plasma membrane level to the nuclear- and lower plasma membrane level were accomplished via en external 488-nm ArKr laser with a BS568 line filter to create confocal images and collected in a 10-sec image sequence. Simultaneous scanning using the internal HeNe red 647-nm laser line was used to produce bright-field images of the cells to assess cell viability. No significant bleaching of the fluorescent probe was observed during the course of observations.

RESULTS

Immunoblot analyses revealed significant differences in immunoreactivity for the PKCα and PKCγ isoenzymes after a 48-h treatment of AC or AD fibroblasts with 10 nM βAP(1–40), whereas no changes were observed for the other PKC isoenzymes tested (PKCβ, PKCδ, and PKCε). Distinct dark bands of about 82 kDa for PKCα and 80 kDa for PKCγ were detected with mAbs in all the age-matched controls and the six familial AD and four sporadic AD cell lines. PKCα immunoreactivity was reduced significantly in all AD fibroblasts as compared with the controls before the βAP(1–40) treatment

Table 1. Densometric measurements of Western blot analyses

	AC			AD	
Patient no.	Control	βAP	Patient no.	Control	βAP
PKCα					
AG03652C	1,238.8 + 35*	121.1 + 23*	AG07872	507.3 + 102*	532.9 + 78*
AG07310	1,031.1 + 208*	145.3 + 41*	AG06263A	468.2	399.7
AG06241B	880.5 + 103*	267.5 + 94*	AG06848B	584.5	451.5
AG08044A	1,340.3 + 211*	214.1 + 71*	AG08563A	656.5 + 38*	534.1 + 103
AG07141	1,141.3 + 301*	466.7 + 107*	AG05770D	880.8	799
AG07603A	1,472.3 + 251	330.6 + 122*	AG06838A	664.2	603.2
AG06842B	813.7 + 219*	243 + 100*	AG07377A	575.1	337.8
AG07665A	1,143.9 + 291*	312.2 + 101*	AG08527A	682	538.2
AG04560B	1,871.2 + 437	420.1 + 122*	AG06840B	153.9	117
AG07867	778 + 283	194.7 + 18*	AG08170B	660.8	573.9
PKCγ					
AG03652C	486.3	497.9	AG07872	642.1	129.6
AG07310	841.5	774.4	AG06263A	1,087.5 + 227*	233.4 + 71*
AG06241B	784.1 + 302*	1,006.5 + 201*	AG06848B	894.5 + 318*	249.2 + 102*
AG08044A	2,189.3	2,056.2	AG08563A	1,029.6 + 211*	234.7 + 99*
AG07141	714.8	616.1	AG05770D	1,312.8	202.1
AG07603A	124.6	121	AG06838A	1,751.5 + 171*	323.5 + 38*
AG06842B	1,479.1	1,454.7	AG07377A	448.8 + 118*	184.7 + 41
AG07665A	2,095.1	2,023.8	AG08527A	776.3	132.1
AG04560B	1,781.5	1,849.1	AG06840B	2,115.7	449.7
AG07867	1,211 + 251*	1,174 + 76	AG08170B	2,178	1,002.2

Values are the expression of the optical density of the immunoreactivity obtained from each single cell line. The Table shows the modifications in the immunoreactivity of PKCα or PKCγ from untreated and βAP(1-40)-treated fibroblasts from control (AC) or AD patients.

*Results of the mean ± SEM of two or more experiments per group.

was administered (Table 1). No significant changes in PKCγ immunoreactivity were detected between the nontreated AC and AD groups. Western blot analysis of fibroblasts treated with βAP(1–40) showed a dramatic reduction of PKCα immunoreactivity in all 10 AC cell lines (Fig. 1*A*), whereas no changes were observed in any of the 10 AD cell lines after βAP treatment (Fig. 1*B*). Interestingly, the treatment of the AD fibroblasts with 10 nM βAP(1–40) for 48 h did lead to a significant decrease in PKCγ immunoreactivity in all 10 AD cell lines as compared with the treated controls (Fig. 1*C*). None of those effects were observed in either the AC or AD groups when other βAP fractions [βAP(1–28) or βAP(25–35), βAP(1–42)] were used (data not shown). Quantitative analysis of the bands confirmed the visual observations (Table 1). Scatter plots of each cell line showed little or no overlap between treated and nontreated fibroblasts (Fig. 2) for the AC or AD groups. Statistical analyses showed that the treatment of AC fibroblasts ($n = 10$) with βAP(1–40) led to a 75% ± 11.3 ($P < 0.001$) decrease in PKCα immunoreactivity as compared with the nontreated controls (Fig. 3*A*), but βAP treatment of AD fibroblasts ($n = 10$) did not further affect PKCα immunoreactivity as compared with the nontreated AD cells. On the other hand, fibroblasts from the AD group ($n = 10$) treated with βAP(1–40) showed a 70% ± 24.8 ($P < 0.001$) decrease in PKCγ immunoreactivity as compared with their controls ($n = 10$), but no changes in PKCγ immunoreactivity were observed between treated and nontreated AC fibroblasts ($n = 10$) (Fig. 3*B*). Double-blind tests conducted on two AC and two AD cell lines confirmed all of the above results (data not shown).

To test whether the changes in PKCα and PKCγ immunoreactivity were mediated by proteasome-mediated protein degradation, immunoblot analyses were performed after preincubation of AC or AD fibroblasts with 50 μM of lactacystine (Lacta), a selective proteasome inhibitor, for 1 h before treatment with 10 nM βAP(1–40) for 48 h. Pretreatment with Lacta prevented degradation of PKCα in AC fibroblasts after exposure to βAP(1–40) (Fig. 4*A*). Similarly, PKCγ degradation was blocked by Lacta in AD fibroblasts treated with βAP(1–40) (Fig. 4*B*).

βAP(1–40) effects on PKC were also observed in rat cerebellar and cortical neurons. Western blot analysis showed that the treatment of rat cerebellar granule cells with 10 nM βAP(1–40) for 48 h significantly decreased PKCα (but not PKCγ) immunoreactivity after 4 and 6 days of maturation *in vitro* (DIV). No modifications in either PKCα or PKCγ immunoreactivity were observed at 0 or 2 DIV (Fig. 5*A*). Similarly, PKCα (but not PKCγ) immunoreactivity was reduced in rat cortical neurons at 10 DIV after treatment with 10 nM βAP(1–40) for 48 h (Fig. 5*B*).

Because recent evidence reported that phorbol esters down-regulate PKCα via the ubiquitin/proteasome pathway (39), we exposed AC and AD fibroblasts to 100 nM phorbol 12-myristate 13-acetate (PMA) for 3 h. This treatment, which causes membrane translocation, but not down-regulation of PKC, selectively reversed the effects of βAP(1–40) on PKCα immunoreactivity in AC fibroblasts (Fig. 6). Surprisingly, PMA was not effective in restoring the PKCγ signal after βAP(1–40) treatment in AD fibroblasts (Fig. 7*B*). To test whether phorbol ester-restoring effects on PKCα were mediated by protein synthesis, we incubated AC fibroblast treated with βAP(1–40) with 100 μM cycloheximide (CHX), a protein synthesis inhibitor, for 30 min before exposure to PMA (Fig. 6). Pretreatment with CHX prevented phorbol esters from restoring PKCα immunoreactivity in AC fibroblasts (Fig. 7*A*). Interestingly, the preincubation with 100 μM CHX for 30 min before the

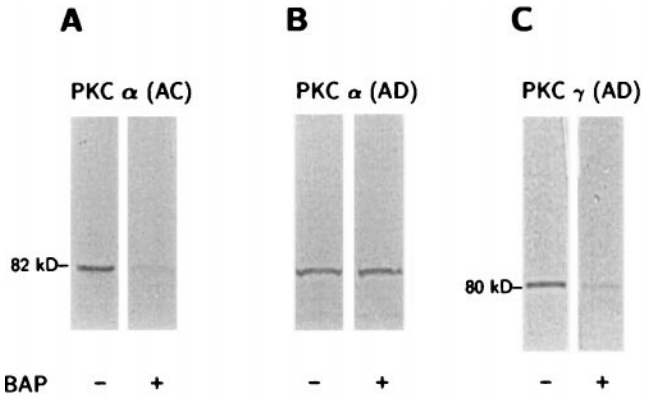

FIG. 1. Effects of βAP on PKCα and PKCγ immunoreactivity. Western blot analyses of monoclonal anti-PKCα or anti-PKCγ immunoreactivities in AC or AD fibroblasts before and after exposure to 10 nM βAP(1–40) for 48 h. (*A*) Visual inspection reveals decreased PKCα immunoreactivity after βAP(1–40) treatment in AC fibroblasts. (*B*) No modifications of PKCα immunoreactivity are visible in AD fibroblasts after treatment with βAP(1–40). (*C*) PKCγ immunoreactivity was decreased after treatment with βAP(1–40) in AD cells.

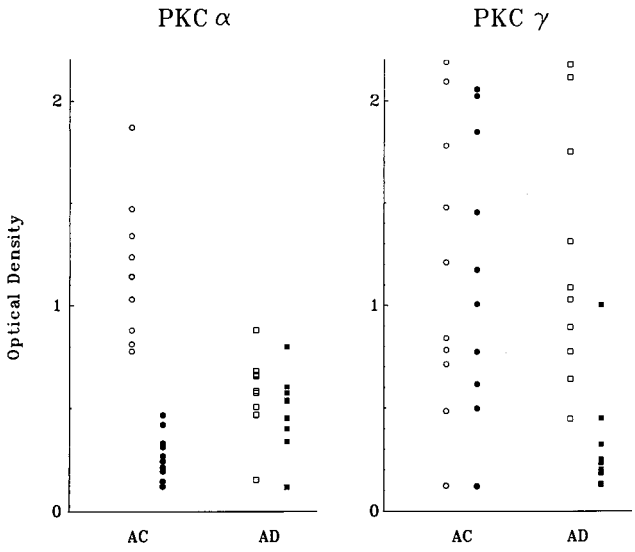

FIG. 2. Scatter plots of optical values from PKCα (*A*) and PKCγ (*B*) immunoreactivities in each cell line (10 aged-matched controls, 4 nonfamilial AD, and 6 familial AD). The graph clearly illustrates the significant differences, with no overlap, between the untreated (○) and treated (●) control (AC) and the untreated (□) and treated (■) AD cell lines.

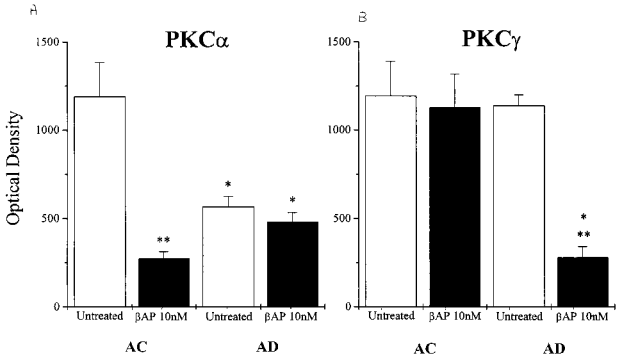

FIG. 3. Bar graphs shows that PKCα (*A*) and PKCγ (*B*) are decreased in fibroblasts from AC fibroblasts and AD fibroblasts, respectively, after treatment with 10 nM βAP(1–40) for 48 h (optical density is an arbitrary unit from densitometric analyses of the immunoreactive bands; values are the mean ± SEM of 10 or more experiments per group; **, $P < 0.001$, significance versus the untreated group; *, $P < 0.001$, significance versus the AC group).

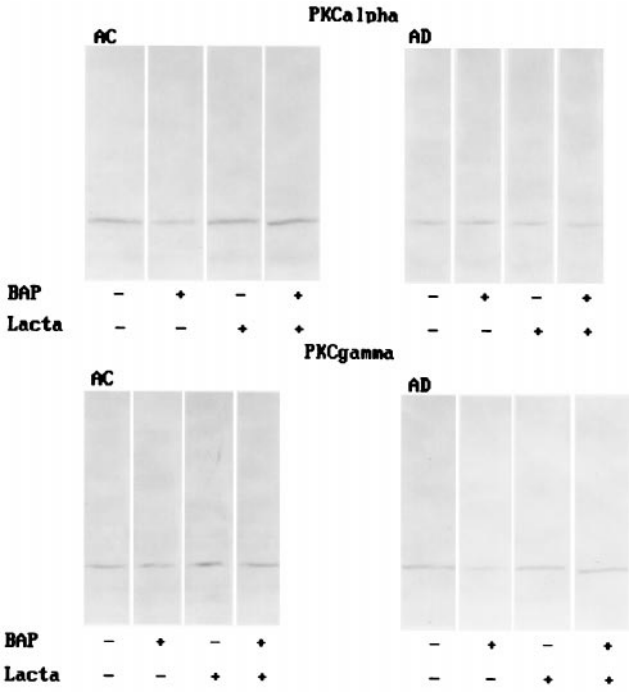

FIG. 4. Western blot analysis of the effects of βAP(1–40) on PKCα immunoreactivity in AC and AD fibroblasts (*A*) and PKCγ immunoreactivity in AC and AD fibroblasts (*B*) after 1 h of preincubation with 50 μM of Lacta. βAP(1–40)-mediated decrease of PKCα immunoreactivity in AC fibroblasts (*A*) and PKCγ immunoreactivity on AD fibroblasts (*B*) is blocked by treatment with Lacta.

addition of βAP(1–40) induced a significant inhibition of the βAP(1–40) effects on PKCα in AC fibroblasts (Fig. 7*A*), suggesting that βAP requires *de novo* protein synthesis to affect PKCα degradation in nonaffected fibroblasts. However, CHX was not effective in preventing βAP(1–40)-mediated PKCγ changes in AD cells (Fig. 7*B*). Confocal microscopy imaging confirmed the Western blot results showing that the PKCα immunofluorescent label localized in the perinuclear area was restored by PKC activation in βAP(1–40)-treated AC fibroblasts (Fig. 8). The effects of PMA also were observed in rat cortical neurons, whereas exposure of βAP(1–40)-treated

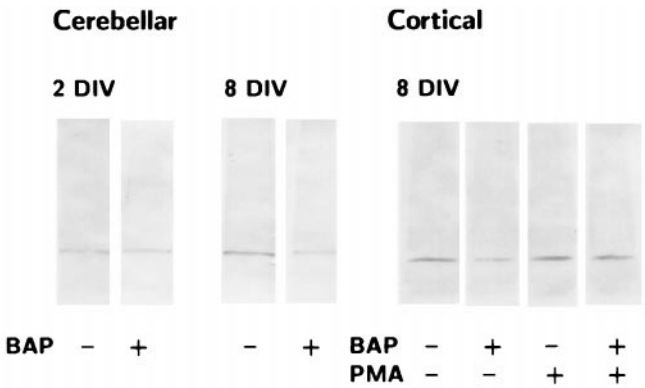

FIG. 5. Western blot analysis of the effects of βAP(1–40) on PKCα immunoreactivity in rat cerebellar granule cells at different days *in vitro* (DIV) (*A*) and rat cortical neurons after 3 h of treatment with 100 nM PMA (*B*). Visual inspection reveals no modifications in PKCα immunoreactivity after βAP(1–40) treatment in rat cerebellar granule cells at 2 days DIV. Decrease of PKCα immunoreactivity is observed after neuronal differentiation at 8 DIV (*Left*). βAP(1–40) reduces PKCα immunoreactivity in rat cortical neurons at 8 DIV, and treatment of βAP(1–40)-treated cortical neurons with PMA restores the PKCα signal (*Right*).

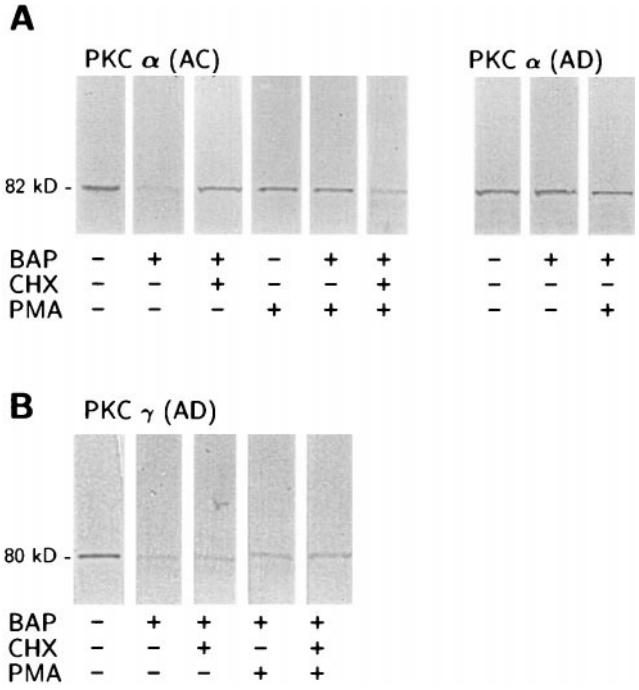

FIG. 6. Western blot analyses of the effects of βAP on PKCα and PKCγ immunoreactivity after treatment with the protein synthesis inhibitor, cycloheximide (CHX), or phorbol ester (PMA). Visual inspection reveals that the decrease of PKCα immunoreactivity after exposure to 10 nM βAP(1–40) for 48 h was blocked by 30 min preincubation with 100 μM CHX (*A*). PKC activation with 100 nM PMA for 3 h restored the PKCα immunoreactive signal in βAP(1–40)-treated AC. PMA effect was blocked by preincubation with CHX. No modifications are visible for PKCα immunoreactivity in the AD group. (*B*) βAP(1–40)-mediated decrease of PKCγ immunoreactivity in AD cells was not affected because preincubation with either CHX or PMA was not able to reverse this effect.

neurons at 10 days DIV to 100 nM PMA for 3 h restored PKCα, but not PKCγ, immunoreactivity (Fig. 5*B*).

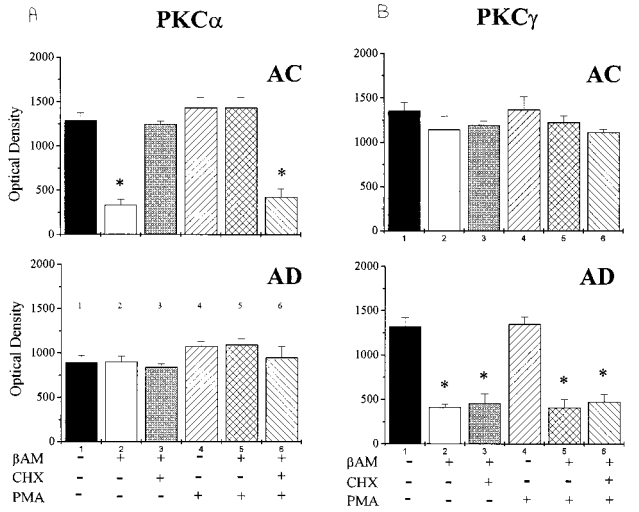

FIG. 7. Bar graphs of densitometric values representing the immunoreactivity following phorbol ester (PMA) and cycloheximide (CHX) treatment in AC (*A*) and AD (*B*) fibroblasts (optical density is an arbitrary unit from densitometric analyses of the immunoreactive bands; values are the mean ± SEM of three experiments per group; *, $P < 0.001$, two-tailed *t* test).

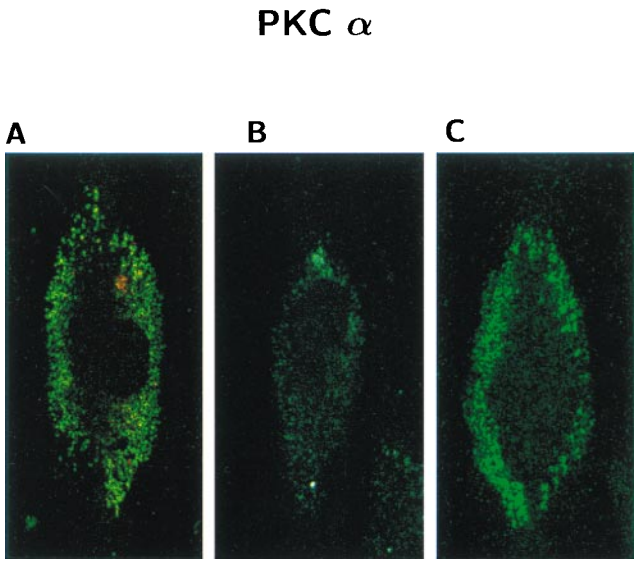

FIG. 8. Confocal microscopy imaging of the effects of βAP(1–40) on PKCα immunofluorescence in AC fibroblasts. (*A*) PKCα immunofluorescence was localized in the perinuclear area of nontreated AC fibroblasts. (*B*) PKCα signal is abolished in AC cell after treatment with 10 nM βAP(1–40) for 48 h. (*C*) PKCα immunofluorescence was almost completely restored after PKC activation with 100 nM PMA for 30 min in βAP-treated AC.

DISCUSSION

These results clearly demonstrate that the soluble form of βAP differentially affects PKCα and PKCγ in normal vs. AD fibroblasts. Previous demonstrations indicated that treatment of rat hippocampal neurons with different fractions of βAP exerts either a neurotropic or neurotoxic effect (21, 22). The βAP concentrations used for our study, although affecting signal transduction by degradation of PKCα in AC cells and PKCγ in the AD cells, do not affect cell viability or induce any neurotoxic effect. Previous observations from this lab indicated that human fibroblasts treated with the same concentrations of βAP(1–40) as those used here induced the blockade of a 113-pS tetraethylammonium-sensitive K+ channel in fibroblasts from AD patients (19). Moreover, treatment of nonaffected human fibroblasts with the same concentrations of βAP(1–40) mimicked the reduction of a GTP-binding/Ca^{2+}-binding protein, calexcitin (cp20), a high-affinity substrate for PKCα, observed in AD fibroblasts (19). Other authors also have reported that the presence of βAP in the culture medium may selectively alter cell metabolism in Alzheimer's tissues (15). Nontoxic concentrations of βAP(25–35) have been shown to increase cultured neuron sensitivity to glutamate-mediated neurotoxicity (41). Here we demonstrated that the exposure of normal neuronal or peripheral cells to nanomolar concentrations of soluble βAP(1–40) induced a reduction in PKCα content greater than the one observed for AD tissues.

Previous findings have reported that alterations in PKC isoenzyme distribution observed in the brain of AD patients (42, 43) may be responsible for a dysfunctional regulation of βAP secretion. $PKC\beta_I$-β_{II} and PKCα, but not PKCγ, seem to be altered selectively in the AD brain (42) and possibly involved in different stages of plaque formation (44). Fibroblasts overexpressing PKCα were demonstrated to enhance the cleavage and release of APP (45). Other evidence also suggested that a reduction of the cytosolic content of PKCα in human fibroblasts may be responsible for affecting APP processing (46), possibly regulating βAP formation. Although little or no modifications in the cytosolic rate of PKCγ have been reported in AD tissues (32, 33, 42, 43), we found that βAP induced PKCγ degradation in AD fibroblasts. Interestingly, βAP did not induce any modification in PKCγ content in nonaffected fibroblasts or in cerebellar or cortical neurons, suggesting that the effects of βAP on PKCγ may be selective for those cells that are already physiologically compromised by Alzheimer's disease. Our findings on βAP effects in cultured neurons from mammalian cerebellum and cortex demonstrated that changes in PKCα immunoreactivity occurred only after a critical stage of development had been achieved. Other studies conducted on rat hippocampal neurons or mouse cortical neurons suggested that aging and cell differentiation help determine βAP effects (21–24, 41, 47) on PKC.

Recent observations demonstrated that phorbol ester-mediated down-regulation of PKCα and PKCε in human fibroblasts occur via the ubiquitin/proteasome pathway (40). Our results demonstrated that βAP-mediated PKCα and PKCγ degradation was blocked by the selective proteasome inhibitor, Lacta, suggesting that in human fibroblasts βAP effects on protein degradation may be mediated by a ubiquitination process. Several reports indicated that PKC activation by phorbol esters increases APP secretion via a nonamyloidogenic pathway (32, 33, 48–51) and decreases βAP secretion (52–54). We found that the treatment of AC fibroblasts with PMA selectively reversed the effects of βAP(1–40) on PKCα immunoreactivity, an effect that was blocked by the presence of CHX. Conversely, activation of PKC was not able to restore the PKCγ signal in the Alzheimer's-diseased fibroblasts. These results suggest that the presence of βAP may induce a defective regulation of PKC correlated with specific PKCα alterations in normal cells and that this process may be mediated at the level of *de novo* protein synthesis. In fact, inhibition of protein synthesis in control fibroblasts reversed the effect of βAP on PKCα degradation, also suggesting the requirement of *de novo* protein synthesis for βAP activity. Because a reduced PKC phosphorylating activity and a lower affinity of phorbol ester binding were detected in AD fibroblasts (32, 33), it is likely that the inability of phorbol esters to reverse the effect of βAP on PKCγ in AD fibroblasts may be caused by constitutive damage provoked by increased circulating levels of βAP in Alzheimer's disease.

In conclusion, these findings represent evidence of a selective effect of βAP on PKC regulation in human cells, suggesting possible new research directions for early diagnosis of Alzheimer's disease and protection of neuronal cells against β-amyloid toxicity, perhaps in an early stage of the disease.

1. Katzman, R. (1986) *N. Eng. J. Med.* **314,** 964–973.
2. Bush, A. I., Beyreuther, K. & Master, C. L. (1992) *Pharmacol. Ther.* **56,** 97–117.
3. Wallace, M. A. (1994) *Biochim. Biophys. Acta* **1227,** 183–187.
4. Gibson, G., Martins, R., Blass, J. & Gandy, S. (1996) *Life Sci.* **59,** 477–489.
5. Cai, X. D., Golde, T. E. & Younkin, S. G. (1993) *Science* **259,** 514–516.
6. Nilsson, E., Alafuzoff, I., Blennow, K., Blomgren, K., Hall, C. M., Janson, I., Karlsson, I., Wallin, A., Gottfries, C. G. & Karlsson, J. O. (1990) *Neurobiol. Aging* **11,** 425–431.
7. Colvin, R. A., Bennett, J. W., Colvin, S. L., Allen, R. A., Martinez, J. & Miner, G. D. (1991) *Brain Res.* **543,** 139–147.
8. Saito, K., Elce, J. S., Hamos, J. E. & Nixon, R. A. (1993) *Proc. Natl. Acad. Sci. USA* **90,** 2628–2632.
9. Huang, H. M., Toral-Barza, L., Sheu, K.-F. R. & Gibson, G. E. (1994) *Neurochem. Res.* **19,** 89–95.
10. Etcheberrigaray, R., Ito, E., Oka, K., Nelson, T. J., McPhie, D. L., Tofel-Grehl, B., Gibson, G. E. & Alkon, D. L. (19934) *Proc. Natl. Acad. Sci. USA* **90,** 8209–8213.
11. Ito, E., Oka, K., Etcheberrigaray, R., Nelson, T. J., McPhie, D. L., Tofel-Grehl, B., Gibson, G. E. & Alkon, D. L. (1994) *Proc. Natl. Acad. Sci. USA* **91,** 534–538.
12. Arispe, N., Rojas, E. & Pollard, H. B. (1993) *Proc. Natl. Acad. Sci. USA* **90,** 567–571.

13. Hadcock, J. R., Port, J. D. & Malbon, C. C. (1991) *J. Biol. Chem.* **266,** 11915–11922.
14. Huang, H. M. & Gibson, G. E. (1993) *J. Biol. Chem.* **268,** 14616–14621.
15. Bruel, A., Cherqui, G., Columelli, S., Margelin, D., Roudier, M., Sinet, P. M., Prieur, M., Perignon, J. L. & Delabar, J. (1991) *Neurosci. Lett.* **133,** 89–92.
16. Mullan, M., Houldon, H., Windelspecht, M., Fidani, L., Lombardi, C., Diaz, P., Rossor, M., Crook, R., Hardy, J., Duff, K., *et al*. (1994) *Nat. Genet.* **2,** 340–342.
17. Citron, M., Vigo-Pelfrey, C., Teplow, D. B., Miller, C., Schenk, D., Johnston, J., Winblad, B., Venizelos, N., Lannfelt, L. & Selkoe, D. J. (1994) *Proc. Natl. Acad. Sci. USA* **91,** 11993–11997.
18. Johnston, J. A., Cowburn, R. F., Norgren, S., Wiehager, B., Venizelos, N., Winblad, B., Vigo-Pelfrey, C., Schenk, D., Lannfelt, L. & O'Neill, C. (1994) *FEBS Lett.* **354,** 274–278.
19. Etcheberrigaray, R., Ito, E., Kim, C. & Alkon, D. L. (1994) *Science* **264,** 276–279.
20. Kim, C., Han, Y. F., Etcheberrigaray, R., Nelson, T. J., Olds, J. L., Yoshioka, T. & Alkon, D. L. (1995) *Proc. Natl. Acad. Sci. USA* **92,** 3060–3064.
21. Yankner, B. A., Duffy, L. K. & Kirschner, D. A. (1990) *Science* **250,** 279–282.
22. Yankner, B. A. & Mesulam, M. M. (1991) *N. Eng. J. Med.* **325,** 1849–1857.
23. Mattson, M. P., Cheng, B., Davis, D., Bryan, K., Lieberburg, I. & Rydel R. E. (1992) *J. Neurosci.* **12,** 376–389.
24. Mattson, M. P., Barger, S. W., Cheng, B., Lieberburg, I., Smith-Swintosky, V. L. & Rydel, R. E. (1992) *Trends Neurosci.* **16,** 409–415.
25. Cowburn, R. F., Fowler, C. J. & O'Neill, C. (1996) *Acta Neurol. Scand.* **165,** 25–32.
26. Sisodia, S. S., Koo, E. H., Beyreuther, K., Unterbeck, A. & Price, D. L. (1990) *Science* **248,** 492–494.
27. Buxbaum, J. D., Koo, E. H. & Greengard, P. (1990) *Proc. Natl. Acad. Sci. USA* **90,** 9195–9198.
28. Estus, S., Golde, T., Kunishita, T., Blades, D., Lowery, D., Eisen, M., Usiak, M., Qu, X., Tabira, T., Greenberg, B. D. & Younkin, S. G. (1992) *Science* **255,** 726–728.
29. Golde, T. E., Estus, S., Younkin, L. H., Selkoe, D. J. & Younkin, S. G (1992) *Science* **255,** 728–730.
30. Shoji, M., Golde, T. D., Ghiso, J., Cheung, T. T., Estus, S., Shaffer, L. M., Cai, X. D., McKay, D. M., Tintner, R., Frangione, B. & Younkin, S. G. (1992) *Science* **258,** 126–129.
31. Hsiao, K.. Chapman, P., Nilsen, S., Eckman, C., Harigaya, Y., Younkin, S., Yang, F. & Cole, G. (1996) *Science* **274,** 99–102.
32. Van Huyhn, T., Cole, G., Ratzman, R., Huang, K. P. & Saitoh T. (1989) *Arch. Neurol.* **46,** 1195–1199.
33. Govoni, S., Bergamaschi, S., Racchi, M., Battaini, F., Binetti, G., Bianchetti, A. & Trabucchi, M. (1993) *Neurology* **43,** 2581–2586.
34. Tesco, G., Vergelli, M., Amaducci, L. & Sorbi, S. (1993) *Exp. Gerontol.* **28,** 51–58.
35. Favit, A., Nicoletti, F., Scapagnini, U. & Canonico, P. L. (1992) *J. Cerebr. Blood Flow Metab.* **12,** 638–643.
36. Ventra, C., Porcellini, A., Feliciello, A., Gallo, A., Paolillo, M., Mele, E., Avvenimento, V. E. & Schettini, G. (1996) *J. Neurochem.* **66,** 1752–1761.
37. Lane, R. D., Federman, D., Flora, J. L. & Beck, B. L. (1986) *J. Immunol. Methods* **92,** 261–270.
38. Dunbar, B. X. (1994) *Protein Blotting: A Practical Approach* (Oxford Univ. Press, New York).
39. Olds, J. L., Favit, A., Nelson, T. J., Ascoli, G., Gerstein, A., Cameron, M., Cameron, L., Lester, D. S., Rakow, T., De Barry, J., *et al.* (1995) *Dev. Biol.* **172,** 675–682.
40. Lee. H.-W., Smith, L., Pettit, G. R. & Bingham Smith, J. (1997) *Mol. Pharmacol.* **51,** 439–447.
41. Gray, C. W. & Patel, A. J. (1995) *Brain Res.* **691,** 169–179.
42. Shimohama, S., Narita, N., Matsushima, H., Kimura, J., Kameyama, M., Hagiwara, M., Hidaka, H. & Taniguchi, T. (1993) *Neurology* **43,** 1407–1413.
43. Masliah, E., Cole, G., Shimohama, S., Hansen, L., DeTeresa, R., Terry, R. & Saitoh, T. (1990) *J. Neurosci.* **10,** 2113–2124.
44. Masliah, E., Cole, H., Mallory, M., Albright, T., Terry, R. & Saitoh, T. (1991) *J. Neurosci.* **11,** 2759–2767.
45. Slack, B. E., Nitsch, R. M., Livnet, E., Kunz, G. M., Breu, J., Eldar, H. & Wurtman, R. J. (1993) *J. Biol. Chem.* **268,** 21097–21101.
46. Bergamaschi, S., Binetti, G., Govoni, S., Wetsel, W. C., Battaini, F., Trabucchi, M., Bianchetti, A. & Racchi, M. (1995) *Neurosci. Lett.* **201,** 1–4.
47. Koh, J. Y., Yang, L. L. & Cotman, C. W. (1990) *Brain Res.* **533,** 315–320.
48. Buxbaum, J. D., Gandy, S. E., Cicchetti, P., Ehrlich, M. E., Czernik, A. J., Fracasso, R. P., Ramabhdaran, T. V., Unterbeck, A. J. & Greengard, P. (1990) *Proc. Natl. Acad. Sci. USA* **89,** 6003–6006.
49. Gillespie, S. L., Golde, T. E. & Younkin, S. G. (1992) *Biochem. Biophys. Res. Commun.* **187,** 1285–1290.
50. Caporaso, G. L., Gandy, S. E., Buxbaum, J. D., Ramabhradram, T. V. & Greengard, P. (1992) *Proc. Natl. Acad. Sci. USA* **89,** 3055–3059.
51. Loffler, J. & Huber, G. (1993) *Biophys. Res. Commun.* **195,** 97–103.
52. Hung, A. Y., Haass, C., Nitsch, R. M., Qiu, W. Q., Citron. M., Wurtman, R. J., Growdon, J. H. & Selkoe, D. J. (1993) *J. Biol. Chem.* **268,** 22959–22962.
53. Gabuzda, D., Busciglio, J. & Yankner, B. A. (1993) *J. Neurochem.* **61,** 2326–2329.
54. Koo, E. H. (1997) *Mol. Med.* **3,** 204–211.